ISSN 0915-633X

NATIONAL INSTITUTE FOR FUSION SCIENCE

A Rational Function Based Scheme for Solving Advection Equation

F. Xiao and T. Yabe

(Received - June 28, 1995)

NIFS-367 July 1995

RESEARCH REPORT
NIFS Series

NAGOYA, JAPAN

A Rational Function Based Scheme for Solving Advection Equation

Feng XIAO

Department of Electronic Engineering, Faculty of Engineering

Gunma University,

1-5-1 Kiryu, Gunma 376, Japan

Takashi YABE

Department of Energy Sciences, Graduate School at Nagatsuta

Tokyo Institute of Technology

4259 Nagatsuta, Midori-ku, Yokohama 227, Japan

ABSTRACT

A numerical scheme for solving advection equations is presented. The scheme is derived from a rational interpolation function. Some properties of the scheme with respect to convex-concave preserving and monotone preserving are discussed. We find that the scheme is attractive in surpressinging overshoots and undershoots even in the vicinities of discontinuity. The scheme can also be easily swicthed as the CIP(Cubic interpolated Pseudo-Particle) method [1−4] to get a third-order accuracy in smooth region. Numbers of numerical tests are carried out to show the non-oscillatory and less diffusive nature of the scheme.

Keywords : Computational algorithm, advection equation, convex-concave preserving, monotone preserving scheme.

1. Introduction

As one of the most important physical processes in fluid dynamics, advection is conventionally described in terms of differential equation as a first-order hyperbolic type like

$$\frac{\partial f}{\partial t} + \mathbf{u} \cdot \nabla f = 0. \quad (1)$$

with f being the dependent variable and $\mathbf{u}$ the velocity.

As a sophisticated numerical solver for advection equation, the CIP method has been developed since the middle of 1980s. It has been applied to simulations of various physical problems and proved to be well-performing [1-4]. The rudimentary principle of the CIP, which makes the scheme quite different from other advection solvers, is to treat the spatial derivatives of the interpolation function, which serves as free parameters in interpolating procedure, as dependent variables. These additional variables are then calculated by their governing equation derived by applying differential operation to advection equation with respect to spatial independent variables. Hence, the free parameters needed in interpolation are determined from the given differential equation rather than from combinations of the values at dicretised grid knots as those, for example, done with Akima or Cubic Bessel formula[5].

In practical implementation, an attractive advection scheme should be both less diffusive and oscillation free. Many high order schemes have been proposed to reduce the numerical diffusion. However, in the presence of discontinuity or breaking down of smoothness, one is likely to meet overshoots or undershoots by directly applying those high order methods. On the other hands, we often encounter situations where the property of positivity appears to be of most importance. Algorithms which can preserve the topological nature of data have been calling for the interests from investigators. Usually, as applications of a high order scheme, manipulations, such as numerical viscosity, are made to degrade the scheme to be of lower order in the presence of discontinuities to eliminate spurious oscillation. Some of these sort schemes are reviewed in [6].

In constructing a CIP-type scheme, the involved interpolation function is of great importance, and some improvements can be expected by using some prospective interpolation functions. We can hope to construct schemes with some desired properties, like TVD, monotone or non-oscillatory, by making use of a proper function.

In this paper, we present an algorithm for advection equation by employing a rational function. The remarkable character of the scheme is convex-concave preserving and monotone preserving. It makes this method quite desirable for practical implementations where the break-down of positivity from numerically spurious oscillation tends to cause serious problems in calculations or simulated results. The scheme appears also less diffusive in sample calculations.

In section 2, the algorithm is presented and some related properties are discussed. Numbers of numerical tests are given in section 3, and a brief conclusion follows in section 4.

2. The algorithm

For given data $f(x_1), f(x_2), \cdots f(x_i) \cdots f(x_{imax})$ with $x_1 < x_2 < \cdots < x_i < \cdots < x_{imax}$, we construct a piecewise interpolation function $F_i(x)$ to $f(x)$ by limiting the number of free parameters to be 4 on each interval $[x_i, x_{i+1}]$.

The ith function piece $F_i(x)$ is made to satisfy the continuity condition:

$$\begin{cases} F_i(x_i) = f(x_i), & F_i(x_{i+1}) = f(x_{i+1}) \\ F_i'(x_i) = d_i, & F_i'(x_{i+1}) = d_{i+1}; \qquad i = 1, 2, \cdots imax \end{cases} \tag{2}$$

here, $\{d_i\}$ are free parameters used to evaluate the derivatives of the interpolation function $F(x)$ and can be determined by various formula. In the CIP method, $\{d_i\}$ are calculated from a governing relation derived from the original advection equation, and we will use the same concept in this paper.

Our scheme is derived from a piecewise rational function in a form as

$$F_i(x) = R_i(x) = \frac{f(x_i) + A1_i(x - x_i) + A2_i(x - x_i)^2}{1 + B_i(x - x_i)} \tag{3}$$

From condition (2), one reads

$$\begin{cases} A1_i = d_i + f_i B_i \\ A2_i = S_i B_i + (S_i - d_i)\Delta_i^{-1} \\ B_i = [(S_i - d_i)/(d_{i+1} - S_i) - 1]\Delta_i^{-1} \end{cases}$$

where

$$\begin{cases} \Delta_i = x_{i+1} - x_i \\ S_i = (f_{i+1} - f_i)\Delta_i{}^{-1} \\ d_i = (\dfrac{df}{dx})_i \end{cases}$$

When $d_i \le S_i \le d_{i+1}$ or $d_i \ge S_i \ge d_{i+1}$ is not satisfied, $B_i \le -\Delta_i^{-1}$ in (3) is observed, and computation will be broken as the denominator of (3) approaching zero at a point within $[x_i, x_{i+1}]$. Thus, for implementation, we modify (3) as

$$F_i(x) = \frac{f(x_i) + A1_i(x - x_i) + A2_i(x - x_i)^2 + A3_i(x - x_i)^3}{1 + \alpha B_i(x - x_i)} \tag{4}$$

and

$$\begin{cases} A1_i = d_i + f_i \alpha B_i \\ A2_i = S_i \alpha B_i + (S_i - d_i)\Delta_i{}^{-1} - A3_i \Delta_i \\ A3_i = [d_i - S_i + (d_{i+1} - S_i)(1 + \alpha B_i \Delta_i)]\Delta_i{}^{-2} \\ B_i = [|(S_i - d_i)/(d_{i+1} - S_i)| - 1]\Delta_i{}^{-1} \end{cases} \tag{5}$$

$\alpha \in [0, 1]$ is a switching parameter. The new term $A3_i(x - x_i)^3$ is determined in such a way that $A3_i$ vanishes for $(S_i - d_i)/(d_{i+1} - S_i) \ge 0$ with $\alpha = 1$ and recovers the coefficient of $(x - x_i)^3$ term in a cubic interpolation fucntion[1], *i.e.* $A3_i = (d_i + d_{i+1} - 2S_i)\Delta_i{}^{-2}$, for $\alpha = 0$.

We write the one dimensional form of the advection equation (1) as

$$\frac{\partial f}{\partial t} + u\frac{\partial f}{\partial x} = 0. \tag{6}$$

The equation governing $\partial f/\partial x$ can be derived directly from eq.(6) as

$$\partial_t(\partial_x f(x,t)) - u\partial_x(\partial_x f(x,t)) = -\partial_x u(x,t)\partial_x f(x,t) \tag{7}$$

where ∂_x refers to $\partial/\partial x$ and ∂_t to $\partial/\partial t$

Usually, it is convenient to handle the right hand side of (7) in nonadvection phase like the treatment in the CIP which solves equations by time splitting into advection and non-advection phases. Thus then, in advection phase, eq.(6) and

$$\partial_t(\partial_x f(x,t)) - u\partial_x(\partial_x f(x,t)) = 0 \tag{8}$$

need to be dealt with.

When f_i^n and $\partial_x f_i^n$ are known for $i = 1, \cdots i_{max}$ with n denoting the time steps, coefficients $A1_i, A2_i, A3_i$ and B_i can be calculated by (5) , and then, both f_i^{n+1} and $\partial_x f_i^{n+1}$ may be predicted by shifting along the characteristics as

$$f_i^{n+1} = F_i(x_i - u\Delta t) = \frac{f_i^n + A1_i\xi + A2_i\xi^2 + A3_i\xi^3}{1 + \alpha B_i \xi} \tag{9a}$$

and

$$\begin{aligned} \partial_x f_i^{n+1} &= \partial_x F_i(x_i - u\Delta t) \\ &= \frac{A_i + 2A2_i\xi + 3A3_i\xi^2}{1 + \alpha B_i\xi} - \frac{\alpha B_i(f_i^n + A1_i\xi + A2_i\xi^2 + A3_i\xi^3)}{(1 + \alpha B_i\xi)^2} \end{aligned} \tag{9b}$$

where $\xi = -u\Delta t$. Eq.(9) is derived for $u \leq 0$. When $u > 0$, we need only take the places of Δ_i and $i+1$ by $-\Delta_{i-1} = x_{i-1} - x_i$ and $i-1$ in foregoing expressions respectively.

Next, let us state and prove some facts about algorithm (9). By keeping in mind that the scheme is a sort of upwind, without losing generality, we limit our discussions to the case of $u \leq 0$.

PROPOSITION 2.1. *When the switching parameter α is set be zero, algorithm (9) is identical to the CIP method.*

proof. The proof is straightforward by eliminating the terms including α in (9) and comparing the resulting expression with eq. (3) in reference [1].

From PROPOSITION 2.1, we know that the CIP method is a particular case of algorithm (9). By letting $\alpha = 0$, the scheme can be switched to the CIP of the third-order in smooth region. Furthermore, one can recover the first-order upwind scheme by setting $d_i^n = d_{i+1}^n = S_i^n$ instead of (9b). Algorithm (9) provides us a flexible form for a class of polynomial based schemes.

Pertaining to the interpolation function itself, we have

LEMMA 2.1. *Assuming $\alpha = 1$, the interpolation function defined with (3) is retrieved from that defined with (4) if the condition: $d_i \leq S_i \leq d_{i+1}$ or $d_i \geq S_i \geq d_{i+1}$ is satisfied.*

proof. The proof is trivial because the coefficient $A3_i$ vanishes for the addressed condition.

LEMMA 2.2. *Under the condition of* LEMMA 2.1, *we have*

$F_i''(x) \geq 0$ for $d_i \leq d_{i+1}$ and $F_i''(x) \leq 0$ for $d_i \geq d_{i+1}$

in every closed subinterval of $[x_i, x_{i+1}]$.

proof. With LEMMA 2.1, by considering function $F_i(x)$ defined with (3), we easily arrive at

$$F_i''(x) = \frac{2(d_{i+1} - S_i)^2(S_i - d_i)^2(x - x_i)^2}{[(d_{i+1} - S_i)(x_{i+1} - x) + (S_i - d_i)(x - x_i)]^3}.$$

It states that $F_i''(x) \geq 0$ is always true for $d_i \leq S_i \leq d_{i+1}$, and $F_i''(x) \leq 0$ for $d_i \geq S_i \geq d_{i+1}$.

We, for further discussion, note some concept as

DEFINITION 2.1. *The data* $\{(x_i, f_i, d_i), i = 1, 2, \cdots, imax\}$ *are said to be nondecreasing if* $f_1 \leq f_2 \leq \cdots \leq f_{imax}$ *or nonconcave if* $d_1 \leq S_1 \leq d_2 \leq S_2 \leq d_3 \leq \cdots \leq d_{imax-1} \leq S_{imax-1} \leq d_{imax}$*; or conversely they are said to be nonincreasing if* $f_1 \geq f_2 \geq \cdots \geq f_{imax}$ *or nonconvex if* $d_1 \geq S_1 \geq d_2 \geq S_2 \geq d_3 \geq \cdots \geq d_{imax-1} \geq S_{imax-1} \geq d_{imax}$.

DEFINITION 2.2. *Let a scheme for eq.(6) be in a form as*

$$f^{n+1} = \Re 1(\Delta t, \Delta, f^n, d^n),$$

and

$$d^{n+1} = \Re 2(\Delta t, \Delta, f^n, d^n)$$

with $f^n = \{f_i^n\}$, $d^n = \{d_i^n\}$ and $\Delta = \{\Delta_i\}$.

It is said to be convex-concave preserving if

$$d_1^{n+1} \leq d_2^{n+1} \leq \cdots \leq d_{imax}^{n+1}$$

is always true for given nonconcave data $\{(x_i, f_i^n, d_i^n)\}$, *or*

$$d_1^{n+1} \geq d_2^{n+1} \geq \cdots \geq d_{imax}^{n+1}$$

for nonconvex data $\{(x_i, f_i^n, d_i^n)\}$;

It is said to be monotone preserving if

$$f_1^{n+1} \leq f_2^{n+1} \leq \cdots \leq f_{imax}^{n+1}$$

is always true for given nondecreasing data, or

$$f_1^{n+1} \geq f_2^{n+1} \geq \cdots \geq f_{imax}^{n+1}$$

for nonincreasing data.

The scheme is said to be non-oscillatory if there exists

$$0 \leq \frac{f_i^{n+1} - f_i^n}{f_{i+1}^n - f_i^n} \leq 1, \quad i = 1, 2, \cdots, imax.$$

About the monotone and convex-concave preserving properties of a given scheme, we address an obvious fact as

LEMMA 2.3. *A scheme for linear advection equation is monotone preserving for nonincreasing data if it is monotone preserving for nondecreasing data; and similarly, a scheme is convex-concave preserving for nonconcave data if it is convex-concave preserving for nonconvex data.*

proof. The proof can be constructed by considering another data set generated as $\{(x_i, p_i = C - f_i), i = 1, 2, \cdots, imax\}$,where $\{f_i\}$ is the original profile and $C \in R$ a real constant. $\{p_i\}$ has opposite properties in monotonicity and convexity to $\{f_i\}$, and a solution for $\{p_i\}$ is equivalent to that for $\{f_i\}$ in sense of the transformation.

Now, with respect to algorithm (9), we can give following results

PROPOSITION 2.2. *Let $\alpha = 1$, under the CFL condition, i.e. $\xi \leq \Delta$, scheme (9) is convex-concave preserving.*

proof. (i). For nonconcave data $\{(x_i, f_i^n, d_i^n), i = 1, 2, \cdots, imax\}$, there exists $d_i^n \leq S_i^n \leq d_{i+1}^n$. From (9b) $\{d_i\}$ are advanced as $d_i^{n+1} = F_i'(x_i + \xi)$. By LEMMA 2.2, and noticing that $F_i'(x_i) = d_i^n \leq F_i'(x_{i+1}) = d_{i+1}^n$, we find that $F_i'(x)$ reachs its minimum at $x = x_i$ and maximum at $x = x_{i+1}$. Since the CFL condition can be interpreted as $x_i \le x_i + \xi \le x_{i+1}$, we obtain the convex-concave preserving preperty as following inequality

$$d_i^n \le d_i^{n+1} \le d_{i+1}^n.$$

(ii). For nonconvex data, we get the result directly by recalling LEMMA 2.3.

PROPOSITION 2.3. *Let $\alpha = 1$, under the CFL condition, scheme (9) is non-oscillatory if the given data $\{(x_i, f_i^n, d_i^n)\}$ satisfies anyone of followings*

- $0 \le d_i^n \le S_i^n \le d_{i+1}^n$ *(nondecreasing and nonconcave),*
- $d_i^n \ge S_i^n \ge d_{i+1}^n \ge 0$ *(nondecreasing and nonconvex),*
- $d_i^n \le S_i^n \le d_{i+1}^n \le 0$ *(nonincreasing and nonconcave),*
- $0 \ge d_i^n \ge S_i^n \ge d_{i+1}^n$ *(nonincreasing and nonconvex).*

proof. The situation of $S_i^n = 0$ is trivial. We only consider that of $S_i^n \ne 0$. From LEMMA 2.1 and (9), we have

$$\begin{aligned}\bar{r}_i \equiv \frac{f_i^{n+1} - f_i^n}{f_{i+1}^n - f_i^n} &= \frac{1}{(1 + B_i\xi)S_i^n\Delta_i}(d_i^n\xi + A1_i\xi^2)\\ &= \frac{1}{(1 + B_i\xi)S_i^n\Delta_i}[d_i^n\xi + S_i^n B_i\xi^2 + \frac{(S_i^n - d_i^n)}{\Delta_i}\xi^2]\end{aligned}$$

(i) For the case of nondecreasing and nonconcave data ($0 \le d_i^n \le S_i^n \le d_{i+1}^n$), we know that $S_i^n - d_i^n \ge 0$, and then by CFL condition, get $(S_i^n - d_i^n)\xi^2/\Delta_i \le (S_i^n - d_i^n)\xi$. Therefore,

$$\bar{r}_i \le \frac{1}{(1 + B_i\xi)S_i^n\Delta_i}[S_i^n\xi(1 + B_i\xi)] = \frac{\xi}{\Delta_i} \le 1$$

meanwhile,

$$\bar{r}_i = \frac{d_i^n(1 - \xi/\Delta_i)\xi + (1 + \Delta_i B_i)S_i^n\xi^2/\Delta_i}{(1 + B_i\xi)S_i^n\Delta_i}.$$

From $d_i^n \ge 0$ and CFL condition, we get

$$\bar{r}_i \ge \frac{1 + B_i\Delta_i}{1 + B_i\xi}(\xi/\Delta_i)^2$$

By (5) one knows that $1 + B_i\Delta_i = |(S_i^n - d_i^n)/(d_{i+1}^n - S_i^n)| \geq 0$ and $1 + B_i\xi = |(S_i^n - d_i^n)/(d_{i+1}^n - S_i^n)|\xi/\Delta_i + (1 - \xi/\Delta_i) \geq 0$, and consequently $\bar{r}_i \geq 0$.

(ii) For the case of nondecreasing and nonconvex data ($d_i^n \geq S_i^n \geq d_{i+1}^n \geq 0$), by $S_i^n - d_i^n \leq 0$ and CFL condition, we get $(S_i^n - d_i^n)\xi^2/\Delta_i \geq (S_i^n - d_i^n)\xi$, and then

$$\bar{r}_i \geq \frac{1}{(1 + B_i\xi)S_i^n\Delta_i}[S_i^n\xi(1 + B_i\xi)] = \frac{\xi}{\Delta_i} \geq 0.$$

On the other hand, $\bar{r}_i$ can be rewritten as

$$\bar{r}_i = 1 + \frac{d_{i+1}^n}{S_i^n}(\xi/\Delta_i - 1) + \frac{(d_{i+1}^n - S_i^n)(1 - \xi/\Delta_i)^2}{(1 + B_i\xi)S_i^n}.$$

Noticing $d_i^n \geq S_i^n \geq d_{i+1}^n \geq 0$ and CFL condition as well, one finds that the last two terms in above expression are less than 0, and then $\bar{r}_i \leq 1$;

(iii) For nonincreasing data we have similar inequalities, or we can complete the proof by LEMME 2.3.

From PROPOSITION 2.3, it is obvious that (9) leads a solution valued between the maximum and minimum within the cell. Thus, no new extremes will be created. As a corollary of PROPOSITION 2.3, we give another fact as

PROPOSITION 2.4. *Let $\alpha = 1$, under the CFL condition, scheme (9) is monotone preserving if the given data is nonconcave or nonconvex.*

Above discussions are undertaken with respect to the interval $[x_i, x_{i+1}]$, and we reach results in a sense of piecwise. For making use of the algorithm, one needs to determine $\{d_i\}$ in advance. One of the choices can be as $d_i^0 = S_i^0, \quad i = 1, 2, \cdots imax$, obviously, the $\{d_i^0\}$ meet the condition of $d_i^0 \leq S_i^0 \leq d_{i+1}^0$ or $d_i^0 \geq S_i^0 \geq d_{i+1}^0$. As calculation proceeds, the data is adapted to fit a rational function. Due to the properties of convex-concave preserving, new extremum is suppressed. We can expect a non-oscillatory profile with the scheme. In the next section, we will give out some numerical tests. The non-oscillatory and less diffusive property is stressed even in the case with extremely irregular initial data.

3. Numerical tests

In this section, we present some sample calculations to test algorithm (9) in a completely rational sense. We refer to the scheme (9) with $\alpha = 1$ as 'completely rational'.

EXAMPLE 3.1. We solve one dimensional linear initial problems as

$$\frac{\partial f}{\partial t} + \frac{\partial f}{\partial x} = 0, \qquad (t, x) \in [0, \infty) \times (-\infty, +\infty); \tag{10}$$

$$f(x, 0) = f^0(x), \qquad x \in (-\infty, +\infty) \tag{11}$$

with following initial conditions

(i)

$$f^0(x) = sin\pi(x+1) \tag{12}$$

(ii)

$$f^0(x) = \begin{cases} 1, & |x| \leq \frac{1}{5} \\ 0, & \text{others} \end{cases} \tag{13}$$

(iii)

$$f^0(x) = \begin{cases} -xsin(3/2\pi x^2), & -1 \leq x < -1/3 \\ |sin(2\pi x)|, & |x| < 1/3 \\ 2x - 1 - sin(2\pi x)/6, & 1/3 \leq x < 1 \\ f^0(x+2). & \end{cases} \tag{14}$$

Equally spaced grid points of $\Delta x = 0.02$ and a CFL number of 0.2 are used.

Initial condition (i) is used to demonstrate the accuracy of the scheme in smooth region. For comparison, we include also the result of the first order upwind scheme in Fig.1. Scheme (9) appears to be highly accurate when applied to smooth data, and no noticeable errors in amplitude are observed. The first order upwind scheme, however, produced a diffused profile due to its low order in accuracy.

Fig.2 illustrates the result from condition (ii). We get a non-oscillation solution by directly using (9). In common, high order schemes tend to generate spurious oscillations in the presence of discontinuities or steep gradients, and many modern high resolution scheme use well specified artificial viscosity to add dissipation near local discontinuities. We fulfill the same task by employing a proper interpolation function.

With condition (iii), we extend the scheme to an extreme case of strong discontinuities, yet the result shows a resolution competitive to many prevalent schemes mentioned in references [7] and [8].

EXAMPLE 3.2. We now turn to a set of two coupled differential equations [9] as

$$\begin{cases} z\dfrac{\partial T_f}{\partial t} + \dfrac{\partial T_f}{\partial x} = T_s - T_f \\ \dfrac{\partial T_s}{\partial t} = T_f - T_s \end{cases} \tag{15}$$

It is a two phase model of the dynamic response of porous media and packed beds systems to any inlet temperature. T_f and T_s are dimensionless temperature of fluid and solid respectively, z the heat capacity ratio of fluid to solid, t dimensionless time and x dimensionless spatial coordinate. Interested readers are recommended to refer to [9] and references therein for physical background of the problem.

For a boundary forcing problem, with $-\infty < t < \infty$ and $T_f = (0,t) = g(t)$, one ends up with a solution as

$$T_f(x,t) = e^{-x}g(t-zx) + e^{-x}x^{1/2}\int_0^\infty \tau^{-1/2}e^{-\tau}I_1[2(x\tau)^{1/2}]g(t-zx-\tau)d\tau \tag{16}$$

and

$$T_s(x,t) = e^{-x}\int_0^\infty e^{-\tau}I_0[2(x\tau)^{1/2}]g(t-zx-\tau)d\tau \tag{17}$$

where I_0 and I_1 are the $0th$ and $1th$ order modified Bessel function of the first kind.

We calculate the numerical solution to the problem by making use of the first-order upwind difference scheme, Lax-Wendroff scheme and algorithm (9). The time varying function is specified as $g(t) = cos(\frac{2}{3}\pi t)$ and the heat capacity ratio $z = 9$. A uniform grid system with $\Delta x = 0.025$ is used. The results at $t = 31.5$ are depicted in Fig.4.

As a process of propagating and damping boundary perturbation, this sample problem is suitable for testing the errors in amplitude and phase speed for a given advection scheme. Upwind scheme, as expected, gives a heavily diffused solution (Fig.4(a)), and few or no variations are observed in the area farther than 3 wave lengths from the forcing source. On the other hand, the Lax-Wendroff scheme appears less encouraging in phase speed. From Fig.4(b), we find an increasing error in phase speed as the distance from forcing source increases, and somewhere, the solution takes on a nearly opposite phase compared with the exact one.

Fig.4(c) shows the result from (9). No significant errors observed in both amplitude and phase speed.

EXAMPLE 3.3. As an application to nonlinear problem, we turn to one dimensional shock tube problem which was originally used by G.A.Sod[10],

$$\begin{aligned} \frac{\partial w}{\partial t} + \frac{\partial f(w)}{\partial x} = 0, \qquad & (t,x) \in [0,\infty) \times (-\infty,+\infty) \\ w(x,0) = w^0(x), \qquad & x \in (-\infty,+\infty) \end{aligned} \tag{18}$$

with following discontinuous initial conditions

$$w^0(x) = \begin{cases} w_L, & x \le 0.5 \\ w_R, & x > 0.5 \end{cases}; \tag{19}$$

where $w = (u, \rho u, \rho E)^T$, $f(w) = (\rho u, p + \rho u^2, u(p+E))^T$; ρ is the density, u the velocity, p the pressure, and E the total energy. For a polytropic gas, there is a relation $p = (\gamma - 1)(E - \frac{1}{2}\rho u^2)$. Numerical test was carried out with $(p_L, \rho_L, u_L) = (1, 1, 0)$ and $(p_R, \rho_R, u_R) = (0.1, 0.125, 0)$. As done in [1], eq.(18) was rewritten in a non-conservative form and computational process is divided into advective phase and non-advective phase in terms of (ρ, u, E). An artificial viscosity based on the Rankine-Hugonoit relation in a form like eq.(29) in [1] was used.

Result at $t = 0.277$ is depicted in Fig.5. We can see, with a proper artificial viscosity, as the CIP method, the present scheme demonstrates ability in capturing both discontinuity and shock wave with a satisfactory accuracy. Compared with the CIP, the scheme (9) tends to produce a less fluctuating solution, even though it appears more diffusive in some senses.

4. Conclusion

We developed a scheme for solving advection equation by making use of a rational function. Numerical tests and theoretical discussions show that the scheme has a high accuracy in smooth region and no oscillation appears in the vicinities of discontinuities or steep gradients. These properties are commonly desirable for all high resolution schemes. Unlike other high-order schemes, our scheme suppresses spurious oscillation by using a convex-concave preserving interpolation function instead of the flux limiters used in many conventional high resolution schemes. The scheme can reach a high order accuracy in smooth region and produce a 'proper' dissipation in the neighbor of discontinuity automatically to eliminate numerical oscillation. It is also noted that the CIP method can be easily recovered from present scheme. Furthermore, the extensions to multi-dimensional version of the scheme is straightforward. The works about 2 and 3 dimension will be presented in a separate paper.

Acknowledgements

This work was carried out under the collaborating research program at the National Institute for Fusion Science of Japan. Thanks are also extended to Mr. Masato Ida at the Department of Energy Sciences of Tokyo Institute of Technology for helpful discussions.

References

[1] T. Yabe and T. Aoki, Comput. Phys. Commun. 60 (1991) 219 .

[2] H.Takewaki and T.Yabe, J. Comput. Phys. 70 (1987) 355.

[3] T. Yabe and T. Ishikawa, P.Y.Wang, T.Aoki, Y.Kadota and F.Ikeda, Comput. Phys. Commun. 66 (1991) 233.

[4] T. Yabe T. Mochizuki and H. Hara, Proceedings of International Conference on Laser Advanced Materials Processing, June 9-12,1991, Nagaoka, Japan.

[5] C. de Boor, A Practical Guide to Splines (Springer-Verlag, New York, 1987).

[6] H.C. Yee, NASA Report TM-89464 (1987).

[7] H.M. Wu and S.L. Yang, A Collection of Papers Presented at The Beijing Workshop on Computational Fluid Dynamics, Institute of Mechanics, Academia Sinica (1990).

[8] C.W. Shu and S.Osher, J. Comput. Phys. 83 (1989) 32.

[9] G. Spiga and M. Spiga, Int. J. Mass Transfer, 24 (1981) 355.

[10] G.A. Sod, J. Comput. Phys. 27 (1978) 1.

Figure captions

Fig.1 : Linear propagation of a sinusoidal wave after 500 time steps ($u \triangle t / \triangle x = 0.2$) with the first-order upwind scheme and the algorithm (9).

Fig.2 : Linear propagation of a square wave after 1000 time steps ($u \triangle t / \triangle x = 0.2$) with the algorithm (9).

Fig.3 : Linear propagation of a profile given by (14) after 500 time steps ($u \triangle t / \triangle x = 0.2$) with the algorithm (9).

Fig.4 : Dynamic response of two phase model to a periodical variation of inlet temperature at $t = 31.5$. (a) with the first upwind scheme, (b) with the Lax-Wendroff scheme, (c) with the algorithm (9).

Fig.5 : Density output at $t = 0.277$ of one dimensional shock tube problem with the algorithm (9).

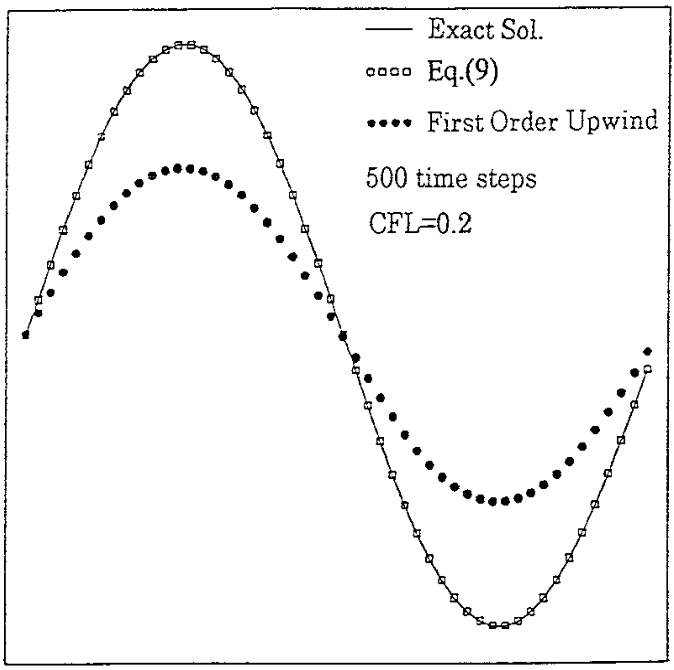

Fig.1

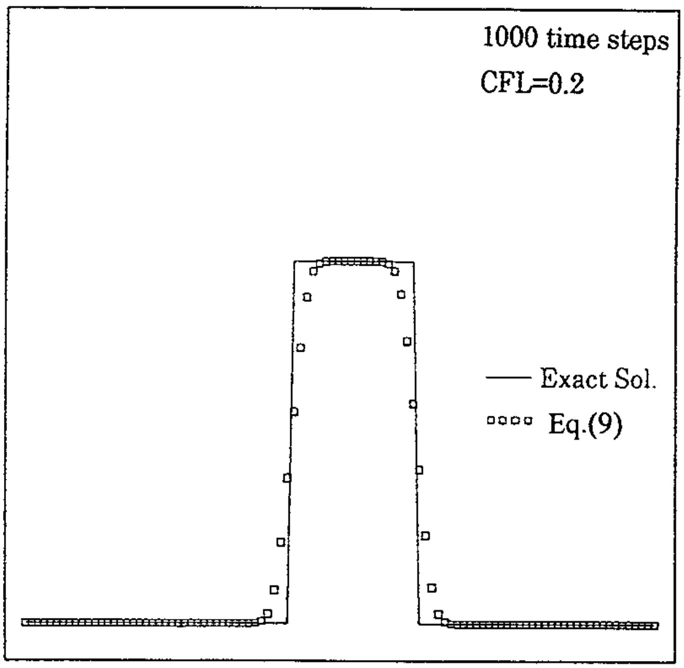

Fig.2

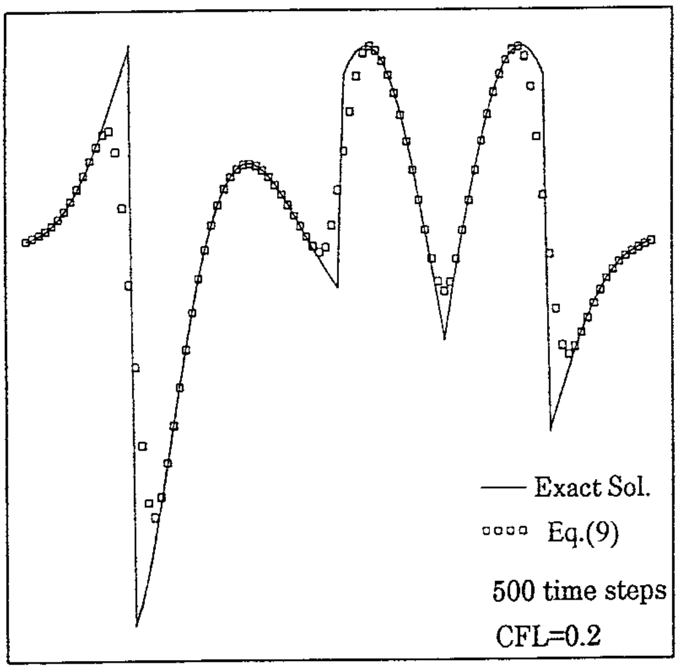

Fig.3

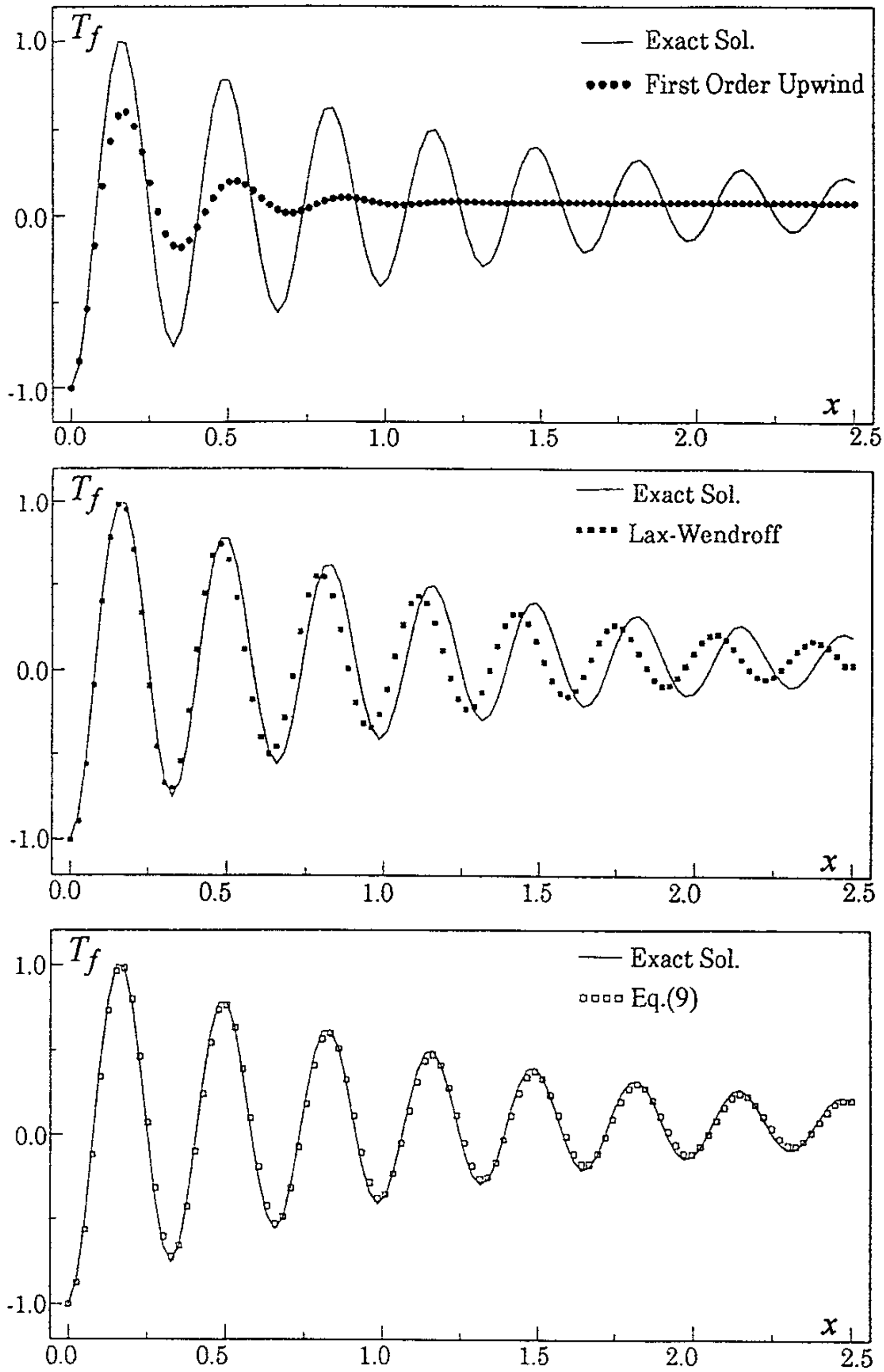

T_f
Exact Sol.
First Order Upwind
1.0
0.0
-1.0
x
0.0
0.5
1.0
1.5
2.0
2.5
T_f
Exact Sol.
Lax-Wendroff
1.0
0.0
-1.0
x
0.0
0.5
1.0
1.5
2.0
2.5
T_f
Exact Sol.
Eq.(9)
1.0
0.0
-1.0
x
0.0
0.5
1.0
1.5
2.0
2.5

Fig.4

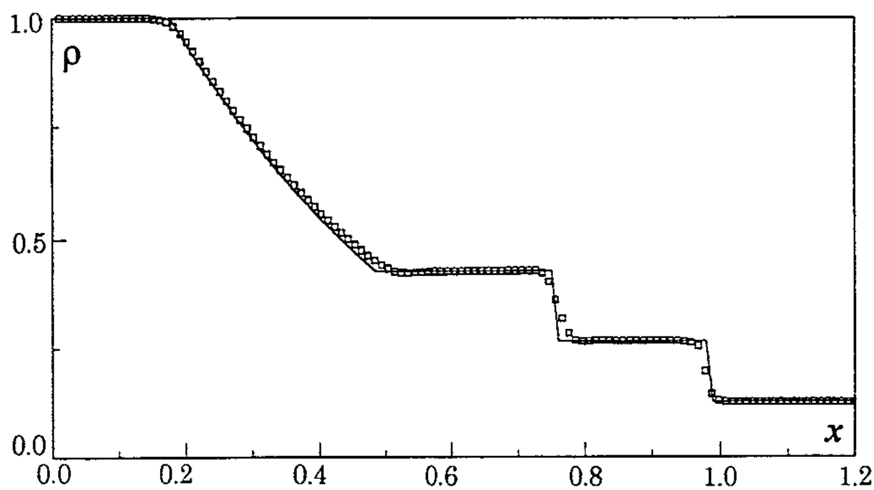

Fig.5

Recent Issues of NIFS Series

NIFS-318 T. Sato and Complexity Simulation Group,
Complexity in Plasma - A Grand View of Self- Organization; Nov. 1994

NIFS-319 Y. Todo, T. Sato, K. Watanabe, T.H. Watanabe and R. Horiuchi,
MHD-Vlasov Simulation of the Toroidal Alfvén Eigenmode; Nov. 1994

NIFS-320 A. Kageyama, T. Sato and The Complexity Simulation Group,
Computer Simulation of a Magnetohydrodynamic Dynamo II: Nov. 1994

NIFS-321 A. Bhattacharjee, T. Hayashi, C.C.Hegna, N. Nakajima and T. Sato,
Theory of Pressure-induced Islands and Self-healing in Three-dimensional Toroidal Magnetohydrodynamic Equilibria; Nov. 1994

NIFS-322 A. Iiyoshi, K. Yamazaki and the LHD Group,
Recent Studies of the Large Helical Device; Nov. 1994

NIFS-323 A. Iiyoshi and K. Yamazaki,
The Next Large Helical Devices; Nov. 1994

NIFS-324 V.D. Pustovitov
Quasisymmetry Equations for Conventional Stellarators; Nov. 1994

NIFS-325 A. Taniike, M. Sasao, Y. Hamada, J. Fujita, M. Wada,
The Energy Broadening Resulting from Electron Stripping Process of a Low Energy Au^- Beam; Dec. 1994

NIFS-326 I. Viniar and S. Sudo,
New Pellet Production and Acceleration Technologies for High Speed Pellet Injection System "HIPEL" in Large Helical Device; Dec. 1994

NIFS-327 Y. Hamada, A. Nishizawa, Y. Kawasumi, K. Kawahata, K. Itoh, A. Ejiri, K. Toi, K. Narihara, K. Sato, T. Seki, H. Iguchi, A. Fujisawa, K. Adachi, S. Hidekuma, S. Hirokura, K. Ida, M. Kojima, J. Koong, R. Kumazawa, H. Kuramoto, R. Liang, T. Minami, H. Sakakita, M. Sasao, K.N. Sato, T. Tsuzuki, J. Xu, I. Yamada, T. Watari,
Fast Potential Change in Sawteeth in JIPP T-IIU Tokamak Plasmas;
Dec. 1994

NIFS-328 V.D. Pustovitov,
Effect of Satellite Helical Harmonics on the Stellarator Configuration;
Dec. 1994

NIFS-329 K. Itoh, S-I. Itoh and A. Fukuyama,
A Model of Sawtooth Based on the Transport Catastrophe; Dec. 1994

NIFS-330 K. Nagasaki, A. Ejiri,

Launching Conditions for Electron Cyclotron Heating in a Sheared Magnetic Field; Jan. 1995

NIFS-331 T.H. Watanabe, Y. Todo, R. Horiuchi, K. Watanabe, T. Sato,
An Advanced Electrostatic Particle Simulation Algorithm for Implicit Time Integration; Jan. 1995

NIFS-332 N. Bekki and T. Karakisawa,
Bifurcations from Periodic Solution in a Simplified Model of Two-dimensional Magnetoconvection; Jan. 1995

NIFS-333 K. Itoh, S.-I. Itoh, M. Yagi, A. Fukuyama,
Theory of Anomalous Transport in Reverse Field Pinch; Jan. 1995

NIFS-334 K. Nagasaki, A. Isayama and A. Ejiri
Application of Grating Polarizer to 106.4GHz ECH System on Heliotron-E; Jan. 1995

NIFS-335 H. Takamaru, T. Sato, R. Horiuchi, K. Watanabe and Complexity Simulation Group,
A Self-Consistent Open Boundary Model for Particle Simulation in Plasmas; Feb. 1995

NIFS-336 B.B. Kadomtsev,
Quantum Telegragh : is it possible?; Feb. 1995

NIFS-337 B.B.Kadomtsev,
Ball Lightning as Self-Organization Phenomenon; Feb. 1995

NIFS-338 Y. Takeiri, A. Ando, O. Kaneko, Y. Oka, K. Tsumori, R. Akiyama, E. Asano, T. Kawamoto, M. Tanaka and T. Kuroda,
High-Energy Acceleration of an Intense Negative Ion Beam; Feb. 1995

NIFS-339 K. Toi, T. Morisaki, S. Sakakibara, S. Ohdachi, T.Minami, S. Morita, H. Yamada, K. Tanaka, K. Ida, S. Okamura, A. Ejiri, H. Iguchi, K. Nishimura, K. Matsuoka, A. Ando, J. Xu, I. Yamada, K. Narihara, R. Akiyama, H. Idei, S. Kubo, T. Ozaki, C. Takahashi, K. Tsumori,
H-Mode Study in CHS; Feb. 1995

NIFS-340 T. Okada and H. Tazawa,
Filamentation Instability in a Light Ion Beam-plasma System with External Magnetic Field; Feb. 1995

NIFS-341 T. Watanbe, G. Gnudi,
A New Algorithm for Differential-Algebraic Equations Based on HIDM; Feb. 13, 1995

NIFS-342 Y. Nejoh,
New Stationary Solutions of the Nonlinear Drift Wave Equation;

Feb. 1995

NIFS-343 A. Ejiri, S. Sakakibara and K. Kawahata,
Signal Based Mixing Analysis for the Magnetohydrodynamic Mode Reconstruction from Homodyne Microwave Reflectometry; Mar.. 1995

NIFS-344 B.B.Kadomtsev, K. Itoh, S.-I. Itoh
Fast Change in Core Transport after L-H Transition; Mar. 1995

NIFS-345 W.X. Wang, M. Okamoto, N. Nakajima and S. Murakami,
An Accurate Nonlinear Monte Carlo Collision Operator; Mar. 1995

NIFS-346 S. Sasaki, S. Takamura, S. Masuzaki, S. Watanabe, T. Kato, K. Kadota,
Helium I Line Intensity Ratios in a Plasma for the Diagnostics of Fusion Edge Plasmas; Mar. 1995

NIFS-347 M. Osakabe,
Measurement of Neutron Energy on D-T Fusion Plasma Experiments; Apr. 1995

NIFS-348 M. Sita Janaki, M.R. Gupta and Brahmananda Dasgupta,
Adiabatic Electron Acceleration in a Cnoidal Wave; Apr. 1995

NIFS-349 J. Xu, K. Ida and J. Fujita,
A Note for Pitch Angle Measurement of Magnetic Field in a Toroidal Plasma Using Motional Stark Effect; Apr. 1995

NIFS-350 J. Uramoto,
Characteristics for Metal Plate Penetration of a Low Energy Negative Muonlike or Pionlike Particle Beam: Apr. 1995

NIFS-351 J. Uramoto,
An Estimation of Life Time for A Low Energy Negative Pionlike Particle Beam: Apr. 1995

NIFS-352 A. Taniike,
Energy Loss Mechanism of a Gold Ion Beam on a Tandem Acceleration System: May 1995

NIFS-353 A. Nishizawa, Y. Hamada, Y. Kawasumi and H. Iguchi,
Increase of Lifetime of Thallium Zeolite Ion Source for Single-Ended Accelerator: May 1995

NIFS-354 S. Murakami, N. Nakajima, S. Okamura and M. Okamoto,
Orbital Aspects of Reachable β *Value in NBI Heated Heliotron/Torsatrons;* May 1995

NIFS-355 H. Sugama and W. Horton,
Neoclassical and Anomalous Transport in Axisymmetric Toroidal Plasmas

with Electrostatic Turbulence; May 1995

NIFS-356 N. Ohyabu
A New Boundary Control Scheme for Simultaneous Achievement of H-mode and Radiative Cooling (SHC Boundary); May 1995

NIFS-357 Y. Hamada, K.N. Sato, H. Sakakita, A. Nishizawa, Y. Kawasumi, R. Liang, K. Kawahata, A. Ejiri, K. Toi, K. Narihara, K. Sato, T. Seki, H. Iguchi, A. Fujisawa, K. Adachi, S. Hidekuma, S. Hirokura, K. Ida, M. Kojima, J. Koong, R. Kumazawa, H. Kuramoto, T. Minami,. M. Sasao, T. Tsuzuki, J.Xu, I. Yamada, and T. Watari,
Large Potential Change Induced by Pellet Injection in JIPP T-IIU Tokamak Plasmas; May 1995

NIFS-358 M. Ida and T. Yabe,
Implicit CIP (Cubic-Interpolated Propagation) Method in One Dimension; May 1995

NIFS-359 A. Kageyama, T. Sato and The Complexity Simulation Group,
Computer Has Solved A Historical Puzzle: Generation of Earth's Dipole Field; June 1995

NIFS-360 K. Itoh, S.-I. Itoh, M. Yagi and A. Fukuyama,
Dynamic Structure in Self-Sustained Turbulence; June 1995

NIFS-361 K. Kamada, H. Kinoshita and H. Takahashi,
Anomalous Heat Evolution of Deuteron Implanted Al on Electron Bombardment; June 1995

NIFS-362 V.D. Pustovitov,
Suppression of Pfirsch-schlüter Current by Vertical Magnetic Field in Stellarators; June 1995

NIFS-363 A. Ida, H. Sanuki and J. Todoroki
An Extended K-dV Equation for Nonlinear Magnetosonic Wave in a Multi-Ion Plasma; June 1995

NIFS-364 H. Sugama and W. Horton
Entropy Production and Onsager Symmetry in Neoclassical Transport Processes of Toroidal Plasmas; July 1995

NIFS-365 K. Itoh, S.-I. Itoh, A. Fukuyama and M. Yagi,
On the Minimum Circulating Power of Steady State Tokamaks; July 1995

NIFS-366 K. Itoh and Sanae-I. Itoh,
The Role of Electric Field in Confinement; July 1995